Cancer Research

Nuclear ErbB2 Enhances Translation and Cell Growth by Activating Transcription of Ribosomal RNA Genes

Long-Yuan Li, Hsiuyi Chen, Yi-Hsien Hsieh, et al.

Cancer Res 2011;71:4269-4279. Published OnlineFirst May 9, 2011.

Published OnlineFirst May 9, 2011; DOI:10.1158/0008-5472.CAN-10-3504

Tumor and Stem Cell Biology

Cancer Research

Nuclear ErbB2 Enhances Translation and Cell Growth by Activating Transcription of Ribosomal RNA Genes

Long-Yuan Li[1,2,3,4], Hsiuyi Chen[1,2], Yi-Hsien Hsieh[1], Ying-Nai Wang[7], Hsiao-Ju Chu[1,2], Ya-Huey Chen[1], Hui-Yu Chen[1,2], Peng-Ju Chien[1,2], Haou-Tzong Ma[3], Ho-Cheng Tsai[1,2], Chien-Chen Lai[1,5], Yuh-Pyng Sher[1], Huang-Chun Lien[6], Chang-Hai Tsai[1,4], and Mien-Chie Hung[1,2,7]

Abstract

Aberrant regulation of rRNA synthesis and translation control can facilitate tumorigenesis. The ErbB2 growth factor receptor is overexpressed in many human tumors and has been detected in the nucleus, but the role of nuclear ErbB2 is obscure. In this study, we defined a novel function of nuclear ErbB2 in enhancing rRNA gene transcription by RNA polymerase-I (RNA Pol I). Nuclear ErbB2 physically associates with β-actin and RNA Pol I, coinciding with active RNA Pol I transcription sites in nucleoli. RNA interference–mediated knockdown of ErbB2 reduced pre-rRNA and protein synthesis. In contrast, wild-type ErbB2 augmented pre-rRNA level, protein production, and cell size/cell growth, but not by an ErbB2 mutant that is defective in nuclear translocation. Chromatin immunoprecipitation assays revealed that ErbB2 enhances binding of RNA Pol I to rDNA. In addition, ErbB2 associated with rDNA, RNA Pol I, and β-actin, suggesting how it could stimulate rRNA production, protein synthesis, and increased cell size and cell growth. Finally, ErbB2-potentiated RNA Pol I transcription could be stimulated by ligand and was not substantially repressed by inhibition of PI3-K and MEK/ERK (extracellular signal regulated kinase), the main ErbB2 effector signaling pathways. Together, our findings indicate that nuclear ErbB2 functions as a regulator of rRNA synthesis and cellular translation, which may contribute to tumor development and progression. *Cancer Res; 71(12); 4269–79. ©2011 AACR.*

Introduction

Recent studies have made significant advances in understanding the role of translation control in cancer formation. rRNA production by RNA polymerase-I (RNA Pol I), the key component of ribosome biogenesis, is the rate-limiting step for translation/protein synthesis and cell growth. Augmented expression of rRNA is potentially accompanied by the increased protein synthesis and thereby cell growth, which can hasten tumor development. Indeed, it has been reported that rRNA and protein synthesis are elevated in wide varieties of human cancers (1–5). Growing evidence also indicates that many oncoproteins and tumor suppressor proteins can contribute to tumorigenesis through regulation of the activities or the expression level of the elements of the translation apparatus (1–10). Thus, the factors of translation machinery have emerged as potential targets for development of novel anticancer therapeutics (5, 11).

ErbB2 (also termed as HER2 or neu) belongs to the cell-surface ErbB receptor tyrosine kinase (RTK) family, of which its best known function is to convey the extracellular stimuli and activate downstream signaling cascades, such as the MAP kinase pathway, the phosphoinositide 3-kinase (PI3-K) pathway, the phospholipase C pathway, and the STATs pathway, leading to specific cellular responses, including cell proliferation, migration, invasion, adhesion, survival, and differentiation (12). Overexpression of ErbB2 has been detected in many human tumors including breast cancer and shown to correlate with more malignant tumor characteristics, such as enhanced metastasis and poor clinical prognosis in breast cancer patients. Thus, ErbB2 has been used as a prominent target for cancer therapeutic intervention (12, 13). In addition to traditional signaling pathways, compelling evidence shows that RTKs, comprising ErbB family, are present in the nucleus (12–17). The correlation of nuclear RTKs with poor patient survival, tumor grade, and pathologic stage has been observed in multiple cancer types by different groups (15, 18–25). This evidence further highlights the important insights that nuclear RTKs potentially play more aggressive roles during tumor progression. Although it has been known that nuclear RTKs associate with functions in RNA Pol II

Authors' Affiliations: [1]Center for Molecular Medicine, China Medical University Hospital; [2]Graduate Institute of Cancer Biology, [3]Cancer Biology and Drug Discovery Ph.D. Program, China Medical University; [4]Department of Biotechnology, Asia University; [5]Institute of Molecular Biology, National Chung Hsing University, Taichung; [6]Department of Pathology, National Taiwan University, Taipei, Taiwan; and [7]Department of Molecular and Cellular Oncology, The University of Texas M.D. Anderson Cancer Center, Houston, Texas

Note: Supplementary data for this article are available at Cancer Research Online (http://cancerres.aacrjournals.org/).

Corresponding Authors: Long-Yuan Li, Center for Molecular Medicine and Graduate Institute of Cancer Biology, China Medical University Hospital, Taichung 40447, Taiwan. Phone: 886-4-22052121; Fax: 886-4-22333496; E-mail: lyl@mail.cmu.edu.tw and Mien-Chie Hung, Department of Molecular and Cellular Oncology, The University of Texas MD Anderson Cancer Center, 1515 Holcombe Blvd, Houston, TX 77030. Phone: 713-792-3668; Fax: 713-794-3270; E-mail: mhung@mdanderson.org

doi: 10.1158/0008-5472.CAN-10-3504

Published OnlineFirst May 9, 2011; DOI:10.1158/0008-5472.CAN-10-3504

transcriptional regulation, DNA repair, and DNA replication (12–16, 20, 26–32), the biological significance and functions of the nuclear RTKs, including ErbB2, is still far from clear. Our study described herein identified a novel function of nuclear ErbB2 in enhancing cellular translation, and thereby cell growth, which may contribute to tumorigenesis.

Materials and Methods

Cells, antibodies, and chemicals

Cell lines were grown in Dulbecco modified Eagle medium (DMEM)-F-12 containing 10% fetal calf serum. MCF-7, SKBR3, and MDA-MB-231 cells were purchased from ATCC in 2007. Liquid nitrogen stocks were done on receipt. Cells were used for no more than 4 months after being thawed. The antibodies and chemicals used were: anti-ErbB2 (Calbiochem, Thermo Scientific); anti-β-actin, anti-α-tubulin, and mouse immunoglobulin (Ig) G (mIgG; Sigma); anti-RPA194 (Santa Cruz); anti-lamin B (Calbiochem); anti-BrdU (Molecular Probes, Abcam); anti-Akt, anti-phospho (p)-Akt, anti-ERK (extracellular signal regulated kinase), anti-p-ERK, and U0126 (Cell Signaling); BrUTP, α-amanitin, and actinomycin D (Act. D; Sigma); LY294002 (Promega); and Heregulin (HRG; Thermo Scientific). Secondary antibodies were purchased from Santa Cruz Biotechnology and Jackson ImmunoResearch. siRNAs were from Dharmacon (control siRNA and ErbB2 siRNA) and Bio-Rad (β-actin siRNA).

Cellular fractionation and immunoprecipitation

Nuclear and cytoplasmic fractions, single immunoprecipitation (IP), and sequential double IP assays were carried out as described (26, 33). Cellular fractionation was examined with α-tubulin and lamin B antibodies.

Chromatin IPs

The chromatin IPs (ChIP) assay was done by the EZ-ChIP Kit (Millipore) according to the manufacturer's instructions. The immunoprecipitated DNA was extracted and purified for PCR by using primers (rDNA promoter, 5′-GGTATATCTTTCGCTCCGAG-3′ and 5′-AGCGACAGGTCGCCAGAGGA-3′; 28S rRNA, 5′-CGACGACCCATTCGAACGTCT-3′ and 5′-CTCTCCGGAATCGAACCCTGA-3′; ref. 34). PCR products were examined on ethidium-bromide–stained agarose gel. For the sequential double ChIP, the first ChIP products were eluted in 10 mmol/L DTT buffer (30 minutes, 37°C), diluted with 40-fold ChIP lysis buffer, and subjected to a second IP as described before by using indicated antibodies.

Real-time quantitative PCR analysis of pre-rRNA synthesis

Cellular RNA was isolated with Trizol reagent (Invitrogen) and purified by the RNeasy Mini Kit (Qiagen). cDNA was generated from total isolated RNA by random primed reverse transcription (RT) and subjected to real-time quantitative PCR (qPCR) performed in triplicate by SYBR Green and LightCycler 480 System (Roche) with 45S pre-rRNA primers (5′-CTCCGTTATGGTAGCGCTGC-3′ and 5′-GCGGAACCCTCGCTTCTC-3′; ref. 34). The *hGAPDH* (human glyceraldehydes 3-phosphate dehydrogenase) and *β-2-microglobulin* primers were used to normalize the loaded amount of RNA.

Protein synthesis analysis

Equal numbers of cells were incubated in methionine-free DMEM (GIBCO/BRL) medium (30 minutes) and 30 μCi of ^{35}S-methionine (Perkin Elmer) was added to the cells (30 minutes). Cells were lysed in equal amount of lysis buffer as described previously (33) and frozen at −70°C. One microliter of thawed lysate was spotted onto a filter and analyzed by liquid scintillation counting. For analysis of total protein level, equal numbers of cells were lysed in lysis buffer and protein concentration determined by the Bradford method (6).

Flow cytometry and measurement of cell size

Cells were washed, trypsinized, resuspended in 1 mL of PBS, and fixed by adding 4 mL of 99% ethanol (80% final) overnight or stored at −20°C until the time of analysis. The fixed cells were then centrifuged, washed, and incubated (37°C, 30 minutes) in propidium iodide/RNase A solution (10 μg/mL propidium iodide in 0.76 mmol/L sodium citrate at pH 7.0; 250 μg/mL RNase A in 10 mmol/L Tris-HCl and 15 mmol/L NaCl at pH 7.5). To detect the relative cell size, the mean forward scatter height (FSC-H) of the cells was determined by the FACsCaliber machine (Becton Dickinson). Data were then analyzed by using CellQuest software (Becton Dickinson) and WinMDI 2.8 software.

Results

ErbB2 associates with β-actin

In an attempt to understand the functionality of nuclear ErbB2, we set to identify potential nuclear proteins that associate with nuclear ErbB2 in the nucleus. By using proteomic assays, monoclonal ErbB2 antibody–precipitated nuclear lysates were subjected to SDS gel electrophoresis and analyzed by mass spectrometry. Interestingly, β-actin, which has also been shown to localize in the nucleus to modulate gene transcription (34–37), was reproducibly detected, suggesting β-actin might be an ErbB2 associating protein. Indeed, association of ErbB2 with β-actin was detected in multiple ErbB2–expressing breast cancer cell lines by using co-IP assays (Fig. 1A and Supplementary Fig. S1A). Moreover, ErbB2 associated with β-actin both in the cytoplasm and the nucleus (Fig. 1A and Supplementary Fig. S1B). The ErbB2/β-actin colocalization was further supported by the yellow spots in the confocal microscopy data (Fig. 1C). Insets 1 and 2 further show the colocalization in the nucleus. Consecutive confocal planes of the nucleus were also examined to show the nuclear colocalization of ErbB2 and β-actin in another cell line (Fig. 1D and Supplementary Fig. S1C). The merged (yellow) signals of ErbB2 (green) and β-actin (red) were detected in plane 18 (arrows). The β-actin (but not ErbB2) signal was still detected in the nucleus in plane 24 and neither was detected in the nucleus of plane 10. Planes 10 to 24 all cover the nucleus [as evident by 4′, 6 diamidino 2 phenylindole (DAPI) staining], indicating that ErbB2 and β-actin colocalize in the nucleus. Together, the results suggest

Published OnlineFirst May 9, 2011; DOI:10.1158/0008-5472.CAN-10-3504

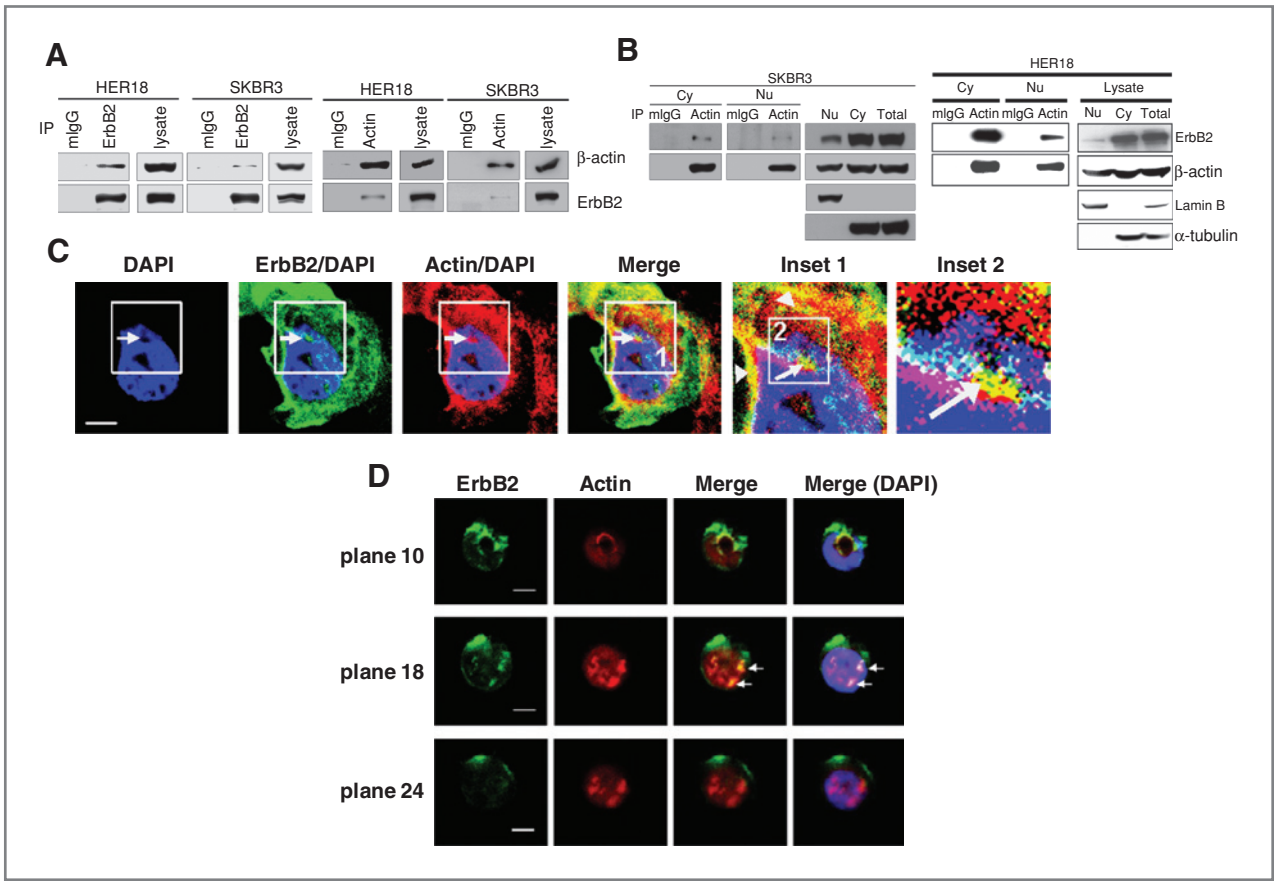

Figure 1. ErbB2 associates with β-actin. A and B, total cell lysates and cytoplasmic (Cy) and nuclear (Nu) lysates from SKBR3 and the MCF-7 stable cell line expressing WT ErbB2 (HER18) were immunoprecipitated by antibodies against ErbB2, β-actin, or mIgG, and then immunoblotted with antibodies as indicated. The cellular fractionation efficiency was also examined by antibodies against α-tubulin and lamin B. C, ErbB2 colocalizes with β-actin in the cytoplasm (inset 1, arrowheads) and the nucleus (insets 1 and 2, arrows) of SKBR3 cells by using confocal analyses of ErbB2 (green), β-actin (red), and nuclei (DAPI staining, blue). The insets 1 and 2 are shown in enlarged images. D, subnuclear localization of the ErbB2 and β-actin in MDA-MB-453 cells by using confocal analyses of ErbB2 (green), β-actin (red), and nuclei (DAPI staining, blue). For confocal microscopy, the cell was dissected into 33 focal planes with a thickness of 0.5 μm each. The nucleus spanned across focal plane 7 to plane 25. The focal planes 10 (top), 18 (middle), and 24 (bottom) are shown here (see Supplementary Figure S1C for details). The middle plan 18 within the nucleus is presented in a particular group of ErbB2 (green)/β-actin (red) complexes whose colocalization is indicated by white arrows in the merged images. Scale bar, 5 μm.

that ErbB2 can associate with β-actin in both the cytoplasm and the nucleus.

ErbB2 forms a complex with β-actin and RNA Pol I

Although nuclear β-actin has been known to be associated with RNA Pol I and is required for RNA Pol I transcription (34) and the nuclear ErbB2 complex was also found to be associated with DNA binding ability and RNA Pol II transcriptional activity (29, 38), we then asked whether ErbB2 might associate with RNA Pol I and be involved in RNA Pol I transcription. Co-IP experiments showed that ErbB2 binds to RNA Pol I in multiple breast cancer cell lines (Fig. 2A and Supplementary Fig. S2A). Association between ErbB2 and RNA Pol I only occurred in the nucleus as revealed by co-IP analyses (Figure 2A, right, and Supplementary Fig. S2B). The colocalization of ErbB2 and Pol I in the nucleus was further supported by confocal microscope data (Fig. 2B, left, and Supplementary Fig. S2C) and sequential confocal image sections (Supplementary Fig. S2D). ErbB2 staining (red) was clearly seen both outside and inside the nucleus (DAPI staining, blue) and RNA Pol I (green) was detected only in the nucleus. In the merged images, the yellow spots indicate the colocalization of ErbB2 and RNA Pol I in the nucleus. To further support the nuclear colocalization, we carried out immunoelectron microscopy (immuno-EM) by using the specific primary antibodies (rabbit anti-ErbB2 and mouse anti-RNA Pol I) followed by incubating with 2 different sized gold particle-labeled secondary antibodies, including those labeling ErbB2 [goat anti-rabbit IgG (rIgG), 5 nm gold] and RNA Pol I (goat anti-mIgG, 1 nm gold). The results showed that ErbB2 and RNA Pol I were both detected and colocalized in the nucleus when the specific primary antibodies against ErbB2 and RNA Pol I were treated (Fig. 2B, right, insets 1 and 2). Without treatment of specific primary antibodies, gold particles were not detected even in the presence of gold particle-labeled secondary antibodies (Fig. 2B, right, inset 3), indicating the specificity of the

Published OnlineFirst May 9, 2011; DOI:10.1158/0008-5472.CAN-10-3504

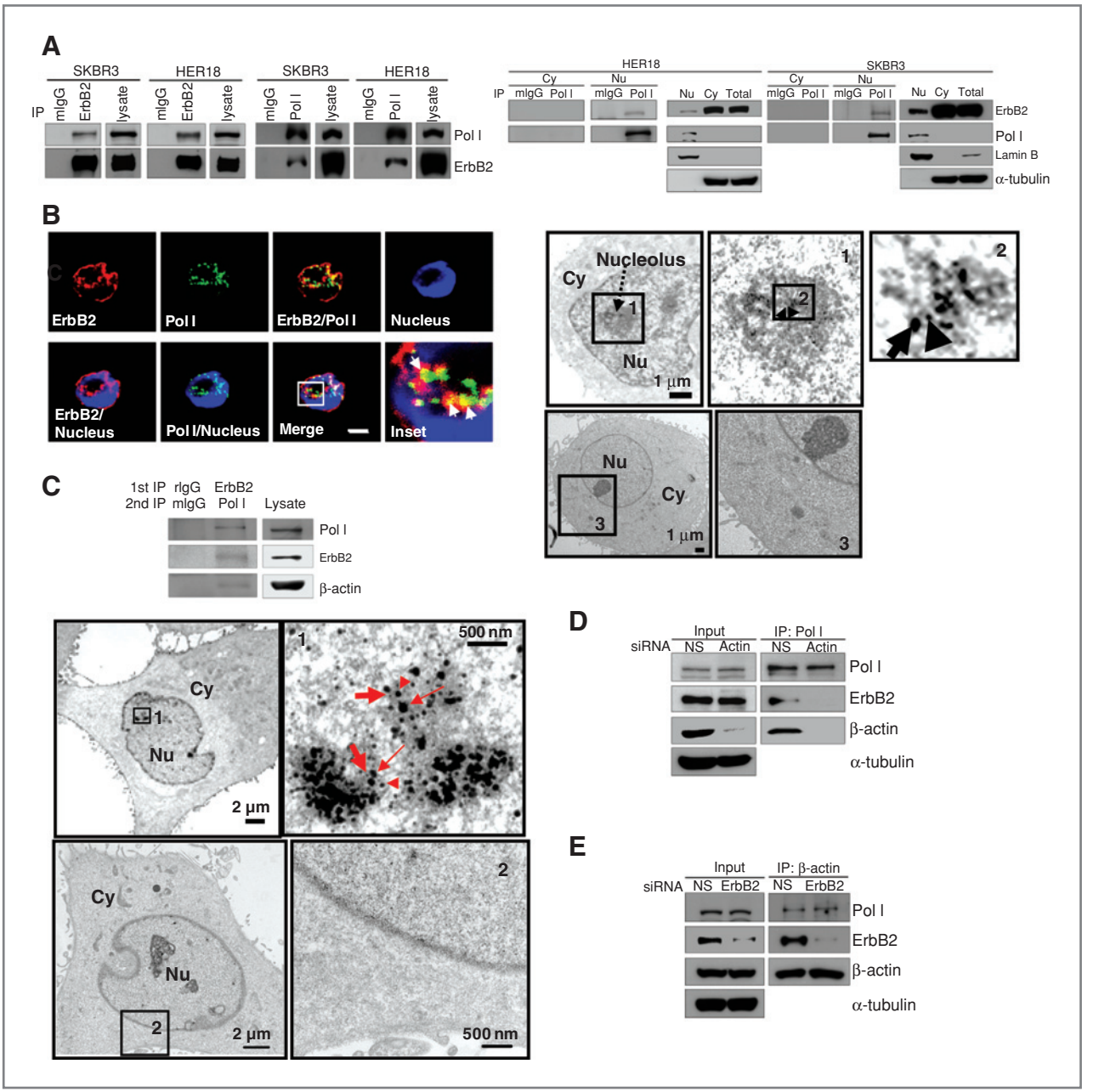

Figure 2. A, ErbB2 associates with RNA Pol I. Total lysate (left) and cytoplasmic and nuclear lysates (right) were IP and analyzed by Western blotting with indicated antibodies. B, left, confocal microscopy of ErbB2 (red) and RNA Pol I (green) colocalization in the nucleus (blue). Inset is enlarged. Scale bar, 5 μm. Right, EM showing colocalization of ErbB2 (solid arrows, 5-nm gold-labeled) and RNA Pol I (arrowheads, 1-nm gold-labeled) in the nucleus. Insets are enlarged. Cy, cytoplasm; Nu, nucleus. Negative control without primary antibody staining; gold particles were not detected even with gold particle-labeled secondary antibodies (lower). C, top, ErbB2 forms complexes with RNA Pol I and β-actin. Cell lysates were primarily IP (1st IP) with anti-ErbB2 or rIgG antibodies, secondarily IP (2nd IP) with antibodies against RNA Pol I or mIgG and analyzed by Western blotting. Bottom, EM shows colocalization of ErbB2 (thin arrows, 25-nm gold-labeled), β-actin (arrowheads, 10-nm gold-labeled), and RNA Pol I (thick arrows, 6-nm gold-labeled) in the nucleus. Insets are enlarged. Negative control as in (B, right). D, total cell lysates from cells transfected with β-actin siRNA or nonspecific (NS) siRNA control were IP with RNA Pol I and subjected to Western blotting as indicated. E, protein extracts from ErbB2 siRNA- or NS siRNA–transfected cells were immunoprecipitated with β-actin and analyzed as in (D).

detected gold particles. It should be mentioned that the ErbB2 and RNA Pol I complex was colocalized in the nucleoli (Fig. 2B, see discussion later). To further explore whether ErbB2, β-actin, and RNA Pol I form a complex, we performed sequential IP assays and showed ErbB2 and RNA Pol I complex with β-actin (Fig. 2C, top), which was further shown by immuno-EM. We used the primary antibodies mouse anti-ErbB2, goat anti-RNA Pol I, and rabbit anti-β-actin followed by

Published OnlineFirst May 9, 2011; DOI:10.1158/0008-5472.CAN-10-3504

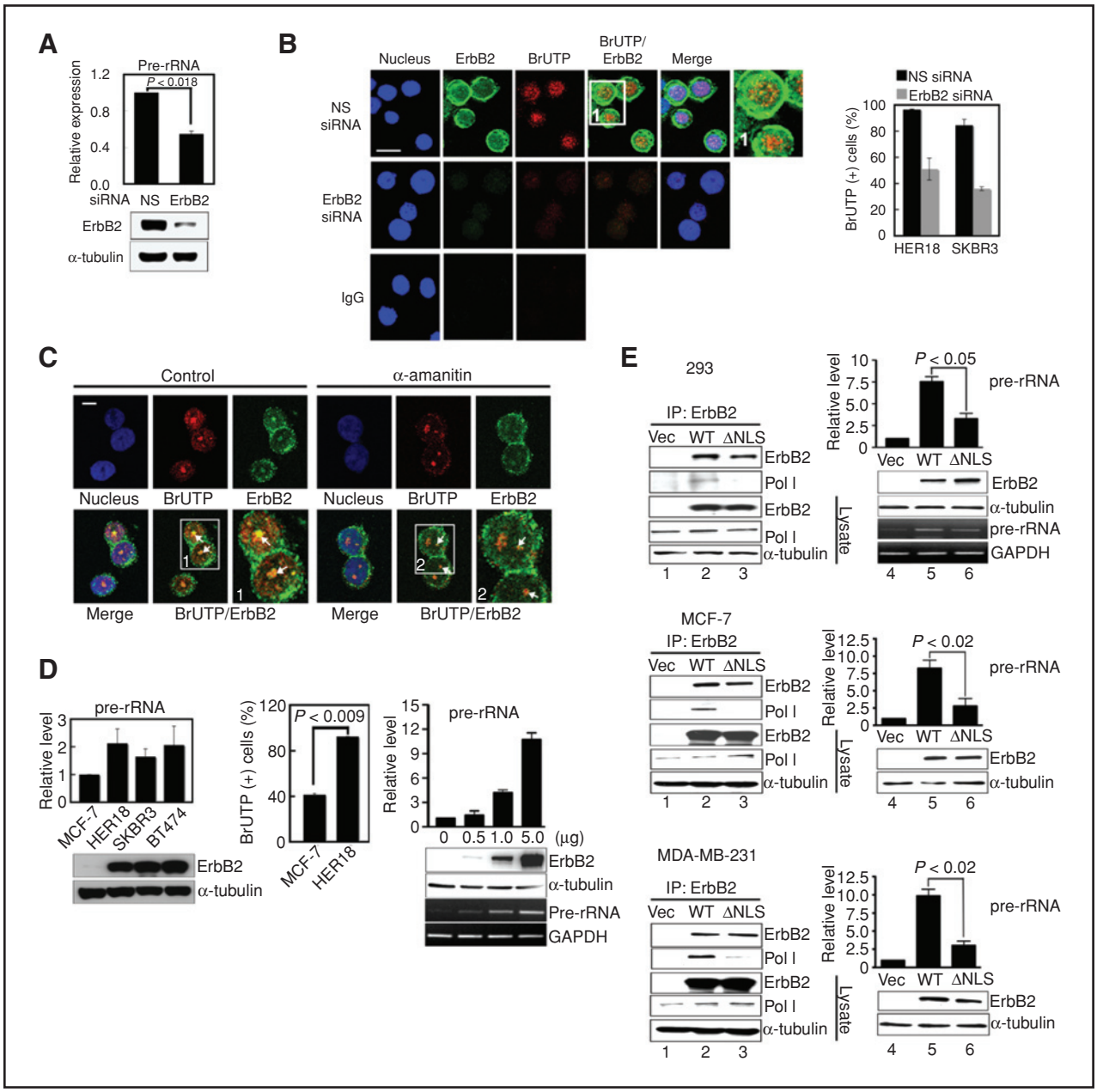

Figure 3. Nuclear ErbB2 increases RNA Pol I transcription *in vivo*. A, cells transfected with ErbB2 or NS siRNAs were assessed for 45S pre-rRNA synthesis by RT-qPCR (top) and ErbB2 protein expression (bottom). Error bar, SD. B, SKBR3 and HER18 cells transfected with ErbB2 siRNA or NS siRNA were subjected to BrUTP incorporation assays of nascent nucleolar RNA and confocal microscopy for ErbB2 (green), BrUTP (red), and nuclei (DAPI, blue). Representative images are from SKBR3 cells. Percentage of BrUTP-positive cells shown as means with SD. C, permeabilized SKBR3 cells were incubated with BrUTP to label active transcription sites with or without α-amanitin. Confocal microscopy was as in (B). D, left, cells were examined for 45S pre-rRNA synthesis (top) and ErbB2 protein (bottom) as in (A). Relative amounts of 45S pre-rRNA shown as means with SD. Middle, BrUTP incorporation assays of nascent nucleolar RNA in MCF-7 and the MCF-7 stable cell line expressing WT ErbB2 (HER18). Percentage of BrUTP-positive cells shown as means with SD. Right, cells transfected with increasing amounts of ErbB2 were measured for 45S pre-rRNA synthesis (top) and ErbB2 protein (middle) as in (A), and RT-PCR of pre-rRNA and internal control GAPDH (bottom). E, transient (293) or stable (MCF-7 and MDA-MB 231) transfectants of WT ErbB2 (WT), ErbB2ΔNLS mutant, or vector (Vec) were assayed for co-IP of ErbB2 with RNA Pol I (left), 45S pre-rRNA synthesis, and ErbB2 protein (right) as in (D, right).

secondary antibodies with gold particles labeling ErbB2 (donkey anti-mIgG, 25 nm), RNA Pol I (donkey anti-goat IgG, 6 nm), and β-actin (donkey anti-rabbit, 10 nm). ErbB2, Pol I, and β-actin were detectable and colocalized in the nucleus as evident from 3 different sized gold particles, which seemed only when primary antibodies against ErbB2, Pol I, and β-actin were applied (Fig. 2C, bottom, inset 1), but did not seem in the negative control without treatment of primary antibodies

Published OnlineFirst May 9, 2011; DOI:10.1158/0008-5472.CAN-10-3504

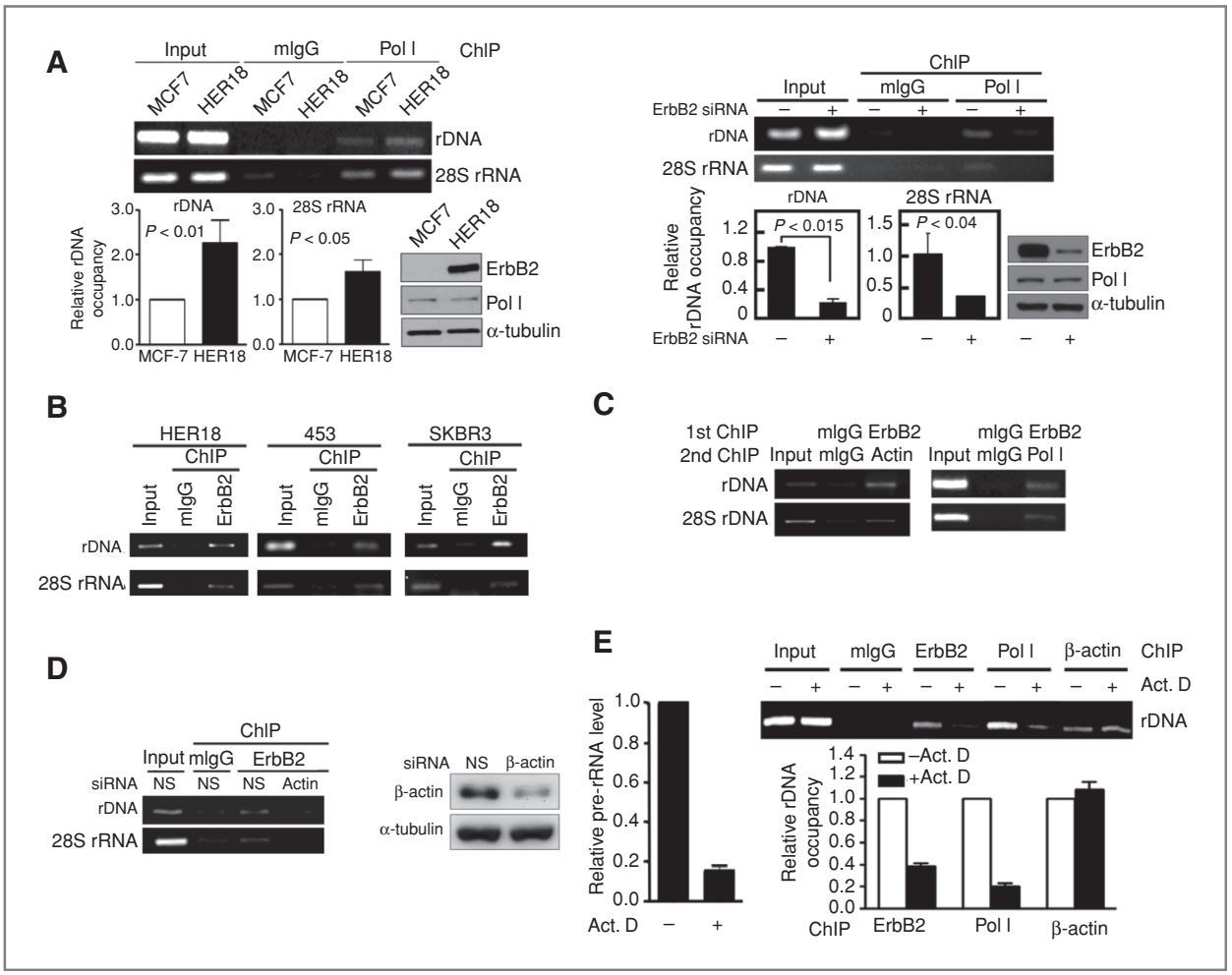

Figure 4. ErbB2 enhances binding of RNA Pol I to rDNA and associates with rDNA during RNA Pol I transcription *in vivo*. A, left, ChIP with RNA Pol I antibody or mIgG of crosslinked chromatin from MCF-7 and HER18 cells. The DNA was amplified by PCR (top) or qPCR (bottom) by using primers specific to the 5′-terminal region of human rDNA or the 28S rRNA coding sequence. The relative rDNA occupancy of RNA Pol I was determined by normalizing rDNA in the Pol I ChIP with rDNA in the mIgG ChIP, then comparing with that in the input chromatin and shown as mean with SD. *P* value was analyzed by Student's *t* test. Western blot shows protein expression. Right, ChIPs from cells transfected with ErbB2 (+) or NS (–) siRNAs by using RNA Pol I or mIgG antibodies were analyzed as in left. B, crosslinked chromatin from ErbB2-expressing cell lines was immunoprecipitated with antibodies against ErbB2 or mIgG and analyzed as in (A). C, sequential ChIP assays were done with first IP (1st ChIP) by anti-ErbB2 or mIgG and second IP (2nd ChIP) using antibodies against β-actin, RNA Pol I, or mIgG. Chromatin samples were amplified as in (B). D, left, ChIPs from cells transfected with β-actin or NS siRNAs using ErbB2 antibody were analyzed as in (B). Right, knockdown of β-actin. E, ErbB2 expressing cells were treated with (+) or without (–) RNA Pol I inhibitor, Act. D. Pre-rRNA synthesis (left) and rDNA occupancy of ErbB2, RNA Pol I, and β-actin (right) were analyzed by RT-qPCR and ChIP assays, respectively. Bar diagram shows relative rDNA binding levels of ErbB2, RNA Pol I, and β-actin in Act. D–treated cells compared with that in cells without treatment.

(Fig. 2C, bottom, inset 2). Notably, knockdown of β-actin using siRNA impaired the association between ErbB2 and RNA Pol I, indicating that β-actin was required for the association of ErbB2 with RNA Pol I (Fig. 2D). However, siRNA-mediated knockdown of ErbB2 exerted no impact on the association between β-actin and RNA Pol I (Fig. 2E). Taken together, our data show that ErbB2 forms a complex with β-actin and RNA Pol I in the nucleus, raising an interesting question about whether nuclear ErbB2 may involve in RNA Pol I transcription.

Nuclear ErbB2 increases RNA Pol I transcription *in vivo*

To address whether nuclear ErbB2 plays a role in RNA Pol I transcription *in vivo*, pre-rRNA synthesis was assessed by RT-qPCR. Strikingly, siRNA-mediated knockdown of ErbB2 resulted in attenuated synthesis of 45S pre-rRNA in 2 different cell lines (Fig. 3A and Supplementary Fig. S3). Consistently, *in situ* run-on transcription assays also showed that BrU-labeled nascent nucleolar RNA levels were reduced in ErbB2 siRNA–treated cells compared with control cells (Fig. 3B). BrUTP and ErbB2 were also shown to be colocalized in the nucleus (Fig. 3B, inset 1). It should be mentioned that nuclear ErbB2 localized in the nucleoli, where RNA Pol I transcription occurs (Fig. 2B, insets 1 and 2). This was further supported by the colocalization of ErbB2 and the nucleoli-specific marker, fibrillarin (Supplementary Fig. S4). To distinguish ErbB2-mediated RNA Pol I transcription from RNA Pol II and

Published OnlineFirst May 9, 2011; DOI:10.1158/0008-5472.CAN-10-3504

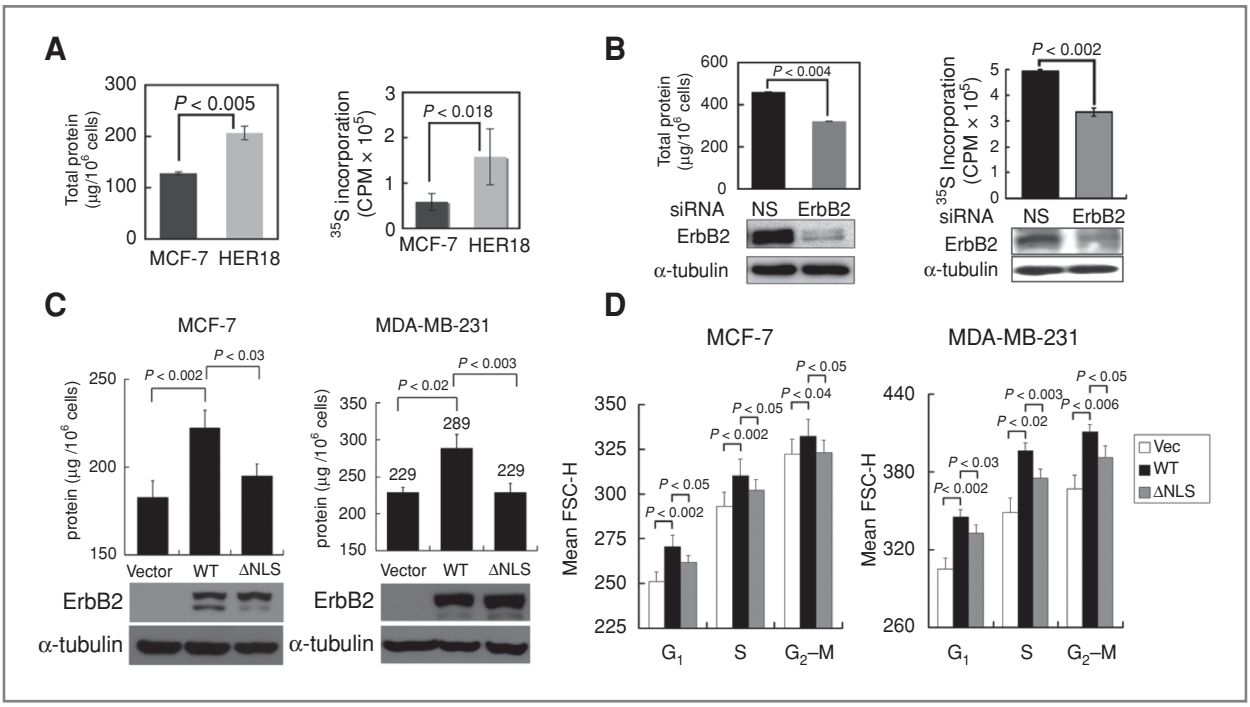

Figure 5. Nuclear ErbB2 increases protein synthesis and cell size. A, left, total protein contents from equal cell numbers of MCF-7 and HER18 cells were determined by the Bradford method. Right, ^{35}S-methionine labeling of protein synthesis in equal cell numbers of MCF-7 and HER18 cells was measured by scintillation counting. B, knockdown of ErbB2 by using siRNA results in decreased protein biosynthesis. Cells transfected with ErbB2 or NS siRNAs were monitored for total protein concentration (left, top) and ^{35}S-methionine incorporation (right, top) as analyzed in (A). ErbB2 protein knockdown was confirmed by Western blotting (bottom). C and D, total protein level and cell size are increased in WT ErbB2 expressing cells but not in cells expressing ErbB2ΔNLS mutant. MCF-7 and MDA-MB-231 cells expressing WT ErbB2, ErbB2ΔNLS mutant, or vector control were assayed for total protein synthesis (C, top) and ErbB2 protein expression (C, bottom) as in (B). Cells were also analyzed by flow cytometry to detect DNA content and cell size of G_1-, S-, and G_2–M phase cells by using the parameter mean FSC-H, which is a measure of relative cell size (D). *P* value was analyzed by Student's *t* test.

Pol III transcription, α-amanitin, a specific inhibitor of RNA Pol II and III transcription was used to treat cells while performing the *in situ* run-on transcription assays. The results showed reduced BrU-labeled nascent nuclear RNA level in the presence of α-amanitin (Fig. 3C); however, the residual BrU-labeled nascent nuclear RNA, which represented Pol I transcribed RNA and is known to be localized in the nucleoli, was still detectable. Overlapping imaging also showed BrUTP and ErbB2 colocalization in the nucleoli, strongly revealing that nuclear ErbB2 resides in the active RNA Pol I transcription sites and may play a novel role in modulation of RNA Pol I transcription apart from its RNA Pol II-associated function (29). In support of this notion, increased expression of ErbB2 also augmented pre-rRNA synthesis (Fig. 3D, left) and BrU-labeled newly synthesized RNA levels (Fig. 3D, middle) compared with cells that express basal levels of ErbB2. Note that HER18 is an ErbB2 stable transfectant of MCF-7 cells. These results were further supported by a dose-dependent enhancement in pre-rRNA synthesis caused by increasing amounts of ErbB2 (Fig. 3D, right). Furthermore, wild-type (WT) ErbB2 with RNA Pol I binding ability greatly enhanced pre-rRNA synthesis (Fig. 3E, lanes 2 and 5). However, ErbB2 whose nuclear localization signal (NLS) was mutated, ErbB2ΔNLS mutant, which is known defect in nuclear translocation (33), exhibited impaired RNA Pol I binding and less enhancement on pre-rRNA synthesis (Fig. 3E, lanes 3 and 6). The results were consistent in all 3 cell lines tested. Together, the results suggest that ErbB2 localizes in the nucleoli and increases RNA Pol I transcription *in vivo*.

ErbB2 enhances binding of RNA Pol I to rDNA and associates with rDNA during RNA Pol I transcription *in vivo*

Recent studies have shown that β-actin and RNA Pol I are associated with the promoter and the coding region of the rDNA (34), which are required for the rRNA gene transcription. To investigate the mechanism underlying ErbB2-mediated augmentation of RNA Pol I transcription, we performed ChIP or quantitative ChIP (qChIP) assays and found that increasing level of ErbB2 caused an enhanced association of RNA Pol I with rDNA promoter and the 28S rRNA transcribed region (Fig. 4A, left). However, knocking down ErbB2 resulted in diminished occupancy of RNA Pol I at rRNA gene (Fig. 4A, right). These data indicate that ErbB2 enhances the binding of RNA Pol I to rDNA. Since ErbB2 associates with β-actin and RNA Pol I *in vivo* (Fig. 1 and Fig. 2), raising the possibility that ErbB2 may be involved in the complex binding to rDNA; indeed, ChIP assays showed that ErbB2, similar to β-actin and RNA Pol I, associated with the 5′-terminal part of rDNA containing promoter and the 28S rRNA transcribed region in multiple ErbB2–expressing breast cancer cell lines (Fig. 4B). These results are in line with colocalization of ErbB2 with the active

Published OnlineFirst May 9, 2011; DOI:10.1158/0008-5472.CAN-10-3504

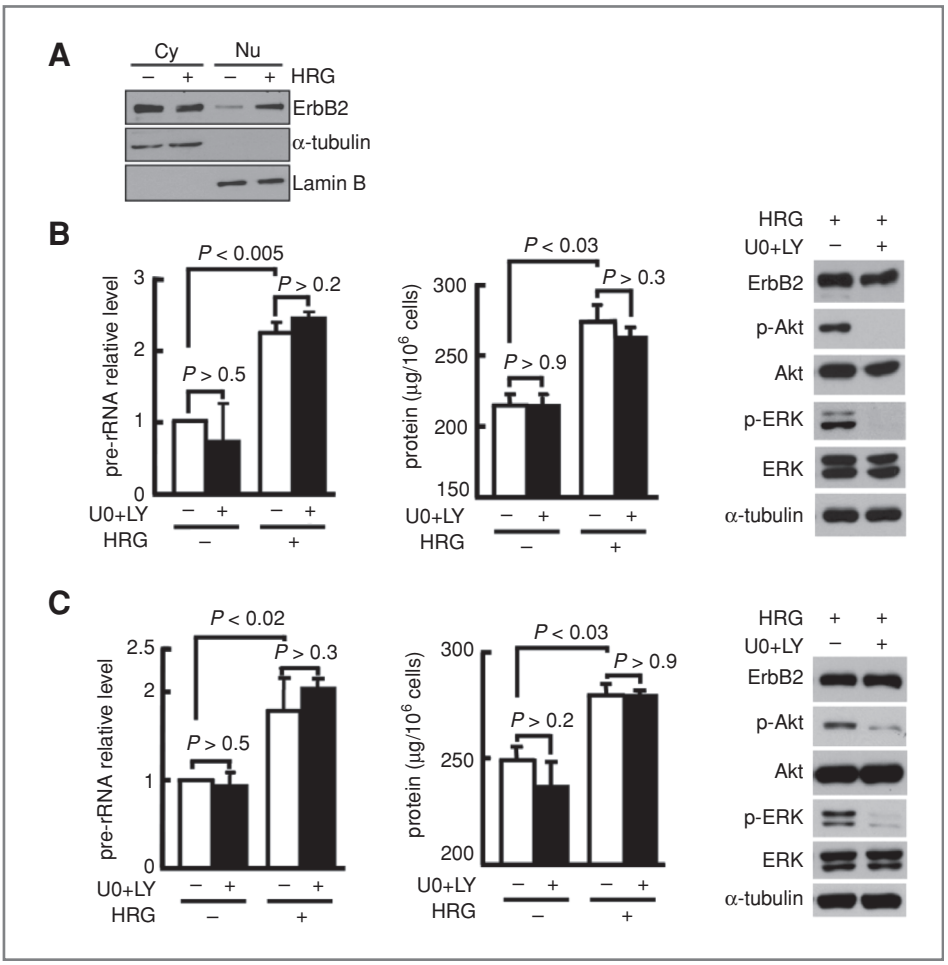

Figure 6. ErbB2-potentiated RNA Pol I transcription can be stimulated by ligand and is independent of PI3-K and ERK activities. A, SKBR3 cells treated with (+) or without (–) HRG (50 ng/mL, 30 minutes) were examined for Western blot of cytoplasmic (Cy) and nuclear (Nu) proteins. B, SKBR3 cells were preincubated with (+) or without (–) 20 μmol/L PI3-K inhibitor LY294002 and 10 μmol/L MEK inhibitor U0126 (U0+LY) for 4 hours, and then treated with (+) or without (–) HRG. The 45S pre-rRNA synthesis (left) and total protein synthesis (middle) were analyzed, as shown in Figures 3A and 5A. Expression of ErbB2, total Akt, p-Akt, total ERK, p-ERK, and α-tubulin proteins was analyzed by Western blotting (right). C, MDA-MB-453 cells treated with (+) or without (–) inhibitors or HRG were analyzed for 45S pre-rRNA synthesis (left), total protein synthesis (middle), and protein expressions (right) as indicated in (B).

RNA Pol I transcription sites within nucleoli (Fig. 3B and C). To further elucidate whether ErbB2 occupies rDNA together with β-actin and RNA Pol I, the sequential ChIP experiments using ErbB2 or control mIgG antibodies for first ChIP followed by a second ChIP with antibodies against β-actin, RNA Pol I, or control mIgG showed that ErbB2 along with β-actin and RNA Pol I simultaneously resides at rDNA (Fig. 4C). In addition, siRNA knockdown of β-actin abrogated the recruitment of ErbB2 to rDNA (Fig. 4D); consistent with the data that β-actin is required for the association of ErbB2 with RNA Pol I (Fig. 2D). Given that ErbB2/β-actin/Pol I co-occupies at rDNA, and β-actin is essential for rDNA occupancy of ErbB2 and RNA Pol I transcription, we next asked whether the association of ErbB2 with rDNA requires ongoing transcription. Inhibition of RNA Pol I transcription using Act. D, which restrains transcription by binding to DNA, resulted in a decreased level of ErbB2 and RNA Pol I at rDNA (Fig. 4E, right) and pre-rRNA synthesis (Fig. 4E, left), indicating that ErbB2 binding to rDNA is dependent on active transcription. Taken together, these results reveal that ErbB2 enhances binding of RNA Pol I to rDNA and associates with rDNA concomitantly with β-actin and RNA Pol I *in vivo*, which is relied on the proceeding transcription. These data support our finding that nuclear ErbB2 increases rDNA transcription by RNA Pol I (Fig. 3).

Nuclear ErbB2 enhances protein synthesis and cell size

It is known that regulation of rRNA transcription by RNA Pol I is an essential cellular process for ribosome biogenesis. The extent of rRNA gene transcription reflects the cellular need for protein synthesis demanded by cell growth. Hence, it is a fundamental step in controlling the capability of protein synthesis, and thereby cell growth (1–5). To validate the biological significance of ErbB2-enhancing RNA Pol I–mediated rRNA synthesis, we therefore analyzed total protein content and protein biosynthetic rate. Total protein level was apparently increased in MCF-7 stable cell line expressing WT ErbB2, HER18, when compared with MCF-7 cell, which expresses basal levels of ErbB2 (Fig. 5A, left). In support of this, ^{35}S-methionine labeling assays also showed that ErbB2 expressing cells exhibited elevated protein biosynthesis (Fig. 5A, right). However, knocking down ErbB2 by siRNA reduced total protein extent and incorporation of ^{35}S-methionine into proteins (Fig. 5B). Moreover, WT ErbB2, but not ErbB2ΔNLS mutant, promoted protein synthesis (Fig. 5C) and increased cell size (Fig. 5D). The increased cell size by ErbB2 is statistically significant and is similar to what has been observed with an increase in the oncoprotein Myc-enhanced cell size by using flow cytometry to detect the relative cell size by mean FSC-H (6, 7). These data are in agreement with the

Published OnlineFirst May 9, 2011; DOI:10.1158/0008-5472.CAN-10-3504

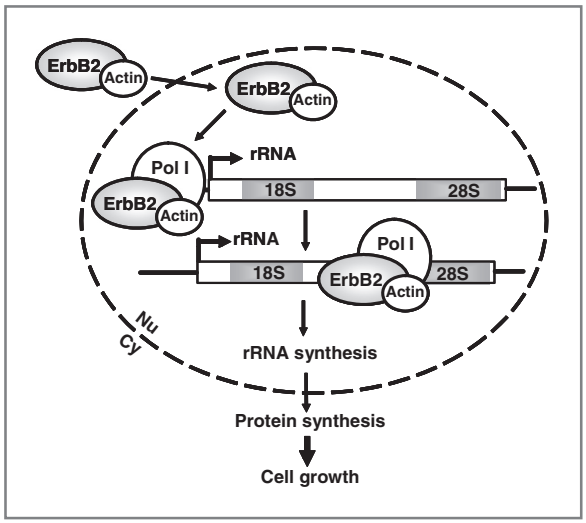

Figure 7. Model depicting the novel function of nuclear ErbB2 in regulation of RNA Pol I–mediated rRNA synthesis.

results that pre-rRNA synthesis was visibly increased in WT ErbB2 expressing cells but not in cells expressing ErbB2ΔNLS mutant (Fig. 3E). Together, these results indicate that nuclear ErbB2 enhances total protein synthesis and cell size, suggesting that nuclear ErbB2 may power cell growth advantage and tumorigenesis by increasing rRNA and protein synthesis.

ErbB2-potentiated RNA Pol I transcription can be stimulated by ligand and is independent of PI3-K and ERK pathways

To further address whether the observed ErbB2-mediated pre-rRNA synthesis is physiologically relevant, we examined the 45S pre-rRNA synthesis in cells that were stimulated by a ligand able to induce ErbB2 nuclear localization (Fig. 6E). Indeed, elevation of ErbB2 nuclear translocation by HRG (refs. 39, 40; Fig. 6A), an ErbB2 activator that induces ErbB2 nuclear translocation–enhanced pre-rRNA synthesis in multiple EerbB2–expressing breast cancer cell lines (Fig. 6B and C, left). Remarkably, 45S pre-rRNA levels were not significantly reduced by inactivation of PI3-K and MEK/ERK, the major ErbB2 downstream signaling cascades. Consistently, total protein content was apparently increased in cells treated with HRG compared with cells without HRG treatment, and was not inhibited by PI3-K inhibitor LY294002 and MEK inhibitor U0126 (Fig. 6B and C, middle). In addition, as shown in Figures 3D and 5A, increased expression of ErbB2 augmented pre-rRNA and total protein synthesis (Figs. 3D, left and 5A), similarly, U0126 and LY294002 also do not affect the over-expressed ErbB2-induced increase in pre-rRNA synthesis and total protein production (Supplementary Fig. S5). Collectively, these results indicate that nuclear ErbB2–augmented RNA Pol I transcription can be stimulated by ligand and is independent of its downstream PI3-K and ERK signaling pathways.

Discussion

Deregulation of translational control can promote cellular transformation. Protein synthesis and the expression of components of the translation machinery are elevated in cancers and contribute to tumorigenesis (1–5, 7). Here, we show that nuclear ErbB2 promotes binding of RNA Pol I to rDNA, co-occupies the rRNA gene with β-actin and RNA Pol I, and stimulates rRNA production and protein translation independently of traditional ErbB2 downstream PI3-K and ERK signalings, suggesting that nuclear ErbB2 may contribute to oncogenesis by upregulating total cellular translation. rRNA synthesis by RNA Pol I plays a critical role in production of mature ribosomes that are central protein synthesis machinery of the cells. Perturbation of RNA Pol I activity as well as rRNA and protein biosynthesis (i.e., translation control) by oncoproteins such as Myc or tumor suppressors p53, RB, and ADP ribosylation factor has been reported to be associated with tumor development (1, 2, 7–10). The capability of Myc to increase protein synthesis is necessary for its oncogenic activity (7). In support of this notion, our findings also manifest the importance of nuclear ErbB2–coordinated rRNA and protein synthesis to tumor biology. In addition, although ErbB2 is known to activate both the MAPK and PI3-K pathways and inhibitors of both pathways (such as AZD6244 and MK2206) have been tested in clinical trials, our current report shows that nuclear ErbB2–potentiated RNA Pol I transcription was not suppressed by inhibition of PI3-K and MEK/ERK, increasing the interesting possibility of whether ErbB2-mediated rRNA transcription might contribute to acquired resistance to clinically used inhibitors of the MAPK and PI3-K pathways.

It is worth mentioning that β-actin, which is originally considered as a cytoplasm protein, also exists in the nucleus and has been shown to be involved in diverse nuclear activities including RNA Pol I transcription (34). Our results show that knocking down β-actin by using siRNA impairs association between ErbB2/RNA Pol I and reduces the level of ErbB2 binding to rRNA gene. Whereas inhibition of RNA Pol I transcription using Act. D, which impedes Pol I transcription by reduced binding of Pol I to DNA, decreases the rRNA gene occupancy of ErbB2 and RNA Pol I, but exerts no impact on β-actin binding to rDNA (Fig. 4E), which is consistent with a previous study, showing that association of β-actin with rDNA does not require ongoing transcription (41). These findings suggest that β-actin is necessary but not sufficient for rDNA association of ErbB2, which also depends on active RNA Pol I transcription. Furthermore, ErbB2, similar to RNA Pol I and β-actin (34), occupies both the rDNA promoter and 28S rRNA coding region, implying that ErbB2 may play a role both in early and later stages (likely elongation) of transcription. It should be mentioned that ErbB2 is a tyrosine kinase and the β-actin/RNA Pol I complex contains multiple proteins, it will be interesting to further pursue whether ErbB2 might phosphorylate some components of the β-actin/RNA Pol I complex to affect RNA Pol I transcriptional activity.

Thus, on the basis of our results, we propose a model (Fig. 7), hypothesizing that ErbB2 enhances binding of RNA Pol I to rDNA and co-occupies rDNA together with β-actin and RNA Pol I, progressing along with these factors in early and elongation steps of transcription, expediting rRNA synthesis and protein translation, and thereby promoting cell growth and tumorigenesis. To the best of our knowledge, our discovery for the first time links the nuclear ErbB2 to a novel function in

Published OnlineFirst May 9, 2011; DOI:10.1158/0008-5472.CAN-10-3504

regulating cellular translation and provides insights into the possible mechanism by which nuclear ErbB2 modulates tumor development through enhancing protein translation.

Disclosure of Potential Conflicts of Interest

No potential conflicts of interest were disclosed.

Acknowledgments

We thank S.A. Miller for editing the manuscript.

Grant Support

This work was supported by grants from NSC95-2311-B-039-002, NHRI-EX99-9603BC, DOH99-TD-I-111-TM026, NSC99-3111-B-039-001 (L.-Y. Li), NIH R01 CA109311, DOD COE W81WXH-06-2-2033 (M.-C. Hung), and NSC98-3111-B-039, DOH100-TD-C-111-005, and NSC99-2632-B-039-001-MY3 (M.-C. Hung and L.-Y. Li).

The costs of publication of this article were defrayed in part by the payment of page charges. This article must therefore be hereby marked *advertisement* in accordance with 18 U.S.C. Section 1734 solely to indicate this fact.

Received September 27, 2010; revised April 12, 2011; accepted April 21, 2011; published OnlineFirst May 9, 2011.

References

1. Ruggero D, Pandolfi PP. Does the ribosome translate cancer? Nat Rev 2003;3:179–92.
2. White RJ. RNA polymerases I and III, growth control and cancer. Nat Rev Mol Cell Biol 2005;6:69–78.
3. White RJ. RNA polymerases I and III, non-coding RNAs and cancer. Trends Genet 2008;24:622–9.
4. Lempiainen H, Shore D. Growth control and ribosome biogenesis. Curr Opin Cell Biol 2009;21:855–63.
5. Silvera D, Formenti SC, Schneider RJ. Translational control in cancer. Nat Rev 2010;10:254–66.
6. Iritani BM, Eisenman RN. c-Myc enhances protein synthesis and cell size during B lymphocyte development. Proc Natl Acad Sci U S A 1999;96:13180–5.
7. Barna M, Pusic A, Zollo O, Costa M, Kondrashov N, Rego E, et al. Suppression of Myc oncogenic activity by ribosomal protein haploinsufficiency. Nature 2008;456:971–5.
8. Oskarsson T, Trumpp A. The Myc trilogy: lord of RNA polymerases. Nat Cell Biol 2005;7:215–7.
9. Belin S, Beghin A, Solano-Gonzalez E, Bezin L, Brunet-Manquat S, Textoris J, et al. Dysregulation of ribosome biogenesis and translational capacity is associated with tumor progression of human breast cancer cells. PloS One 2009;4:e7147.
10. van Riggelen J, Yetil A, Felsher DW. MYC as a regulator of ribosome biogenesis and protein synthesis. Nat Rev 2010;10:301–9.
11. Drygin D, Rice WG, Grummt I. The RNA polymerase I transcription machinery: an emerging target for the treatment of cancer. Annu Rev Pharmacol Toxicol 2010;50:131–56.
12. Citri A, Yarden Y. EGF-ERBB signalling: towards the systems level. Nat Rev Mol Cell Biol 2006;7:505–16.
13. Bublil EM, Yarden Y. The EGF receptor family: spearheading a merger of signaling and therapeutics. Curr Opin Cell Biol 2007;19:124–34.
14. Wang SC, Hung MC. Nuclear translocation of the EGFR family membrane tyrosine kinase receptors. Clin Cancer Res 2009:15:6484–9.
15. Lo HW, Hung MC. Nuclear EGFR signalling network in cancers: linking EGFR pathway to cell cycle progression, nitric oxide pathway and patient survival. Br J Cancer 2006;94:184–8.
16. Massie C, Mills IG. The developing role of receptors and adaptors. Nat Rev 2006;6:403–9.
17. Wang YN, Yamaguchi H, Hsu JM, Hung MC. Nuclear trafficking of the epidermal growth factor receptor family membrane proteins. Oncogene 2010;29:3997–4006.
18. Hoshino M, Fukui H, Ono Y, Sekikawa A, Ichikawa K, Tomita S, et al. Nuclear expression of phosphorylated EGFR is associated with poor prognosis of patients with esophageal squamous cell carcinoma. Pathobiology 2007;74:15–21.
19. Xia W, Wei Y, Du Y, Liu J, Chang B, Yu YL, et al. Nuclear expression of epidermal growth factor receptor is a novel prognostic value in patients with ovarian cancer. Mol Carcinog 2009;48:610–7.
20. Lo HW, Xia W, Wei Y, Ali-Seyed M, Huang SF, Hung MC. Novel prognostic value of nuclear epidermal growth factor receptor in breast cancer. Cancer Res 2005;65:338–48.
21. Psyrri A, Yu Z, Weinberger PM, Sasaki C, Haffty B, Camp R, et al. Quantitative determination of nuclear and cytoplasmic epidermal growth factor receptor expression in oropharyngeal squamous cell cancer by using automated quantitative analysis. Clin Cancer Res 2005;11:5856–62.
22. Junttila TT, Sundvall M, Lundin M, Lundin J, Tanner M, Harkonen P, et al. Cleavable ErbB4 isoform in estrogen receptor-regulated growth of breast cancer cells. Cancer Res 2005;65:1384–93.
23. Maatta JA, Sundvall M, Junttila TT, Peri L, Laine VJ, Isola J, et al. Proteolytic cleavage and phosphorylation of a tumor-associated ErbB4 isoform promote ligand-independent survival and cancer cell growth. Mol Biol Cell 2006;17:67–79.
24. Koumakpayi IH, Diallo JS, Le Page C, Lessard L, Gleave M, Begin LR, et al. Expression and nuclear localization of ErbB3 in prostate cancer. Clin Cancer Res 2006;12:2730–7.
25. Hadzisejdic I, Mustac E, Jonjic N, Petkovic M, Grahovac B. Nuclear EGFR in ductal invasive breast cancer: correlation with cyclin-D1 and prognosis. Mod Pathol 2010;23:392–403.
26. Wang SC, Nakajima Y, Yu YL, Xia W, Chen CT, Yang CC, et al. Tyrosine phosphorylation controls PCNA function through protein stability. Nat Cell Biol 2006;8:1359–68.
27. Lin SY, Makino K, Xia W, Matin A, Wen Y, Kwong KY, et al. Nuclear localization of EGF receptor and its potential new role as a transcription factor. Nat Cell Biol 2001;3:802–8.
28. Ni CY, Murphy MP, Golde TE, Carpenter G. Gamma-secretase cleavage and nuclear localization of ErbB-4 receptor tyrosine kinase. Science 2001;294:2179–81.
29. Wang SC, Lien HC, Xia W, Chen IF, Lo HW, Wang Z, et al. Binding at and transactivation of the COX-2 promoter by nuclear tyrosine kinase receptor ErbB-2. Cancer Cell 2004;6:251–61.
30. Sardi SP, Murtie J, Koirala S, Patten BA, Corfas G. Presenilin-dependent ErbB4 nuclear signaling regulates the timing of astrogenesis in the developing brain. Cell 2006;127:185–97.
31. de la Iglesia N, Konopka G, Puram SV, Chan JA, Bachoo RM, You MJ, et al. Identification of a PTEN-regulated STAT3 brain tumor suppressor pathway. Genes Dev 2008;22:449–62.
32. Huo L, Wang YN, Xia W, Hsu SC, Lai CC, Li LY, et al. RNA helicase A is a DNA-binding partner for EGFR-mediated transcriptional activation in the nucleus. Proc Natl Acad Sci U S A 2010;107:16125–30.
33. Giri DK, Ali-Seyed M, Li LY, Lee DF, Ling P, Bartholomeusz G, et al. Endosomal transport of ErbB-2: mechanism for nuclear entry of the cell surface receptor. Mol Cell Biol 2005;25:11005–18.
34. Philimonenko VV, Zhao J, Iben S, Dingova H, Kysela K, Kahle M, et al. Nuclear actin and myosin I are required for RNA polymerase I transcription. Nat Cell Biol 2004;6:1165–72.
35. de Lanerolle P, Johnson T, Hofmann WA. Actin and myosin I in the nucleus: what next? Nat Struct Mol Biol 2005;12:742–6.
36. Grummt I. Actin and myosin as transcription factors. Curr Opin Genet Dev 2006;16:191–6.
37. Percipalle P, Visa N. Molecular functions of nuclear actin in transcription. J Cell Biol 2006;172:967–71.
38. Xie Y, Hung MC. Nuclear localization of p185neu tyrosine kinase and its association with transcriptional transactivation. Biochem Biophys Res Commun 1994;203:1589–98.

Published OnlineFirst May 9, 2011; DOI:10.1158/0008-5472.CAN-10-3504

39. Holmes WE, Sliwkowski MX, Akita RW, Henzel WJ, Lee J, Park JW, et al. Identification of heregulin, a specific activator of p185erbB2. Science 1992;256:1205–10.

40. Bacus SS, Huberman E, Chin D, Kiguchi K, Simpson S, Lippman M, et al. A ligand for the erbB-2 oncogene product (gp30) induces differentiation of human breast cancer cells. Cell Growth Differ 1992;3:401–11.

41. Ye J, Zhao J, Hoffmann-Rohrer U, Grummt I. Nuclear myosin I acts in concert with polymeric actin to drive RNA polymerase I transcription. Genes Dev 2008;22:322–30.

Supplemental Data

Nuclear ErbB-2 Enhances Translation and Cell Growth by activating transcription of rRNA genes

Long-Yuan Li, Hsiuyi Chen, Yi-Hsien Hsieh, Ying-Nai Wang, Hsiao-Ju Chu, Ya-Huey Chen, Hui-Yu Chen, Peng-Ju Chien, Haou-Tzong Ma, Ho-Cheng Tsai, Chien-Chen Lai, Yuh-Pyng Sher, Huang-Chun Lien, Chang-Hai Tsai and Mien-Chie Hung

Materials and Methods

Br-UTP labeling and immunofluorescence microscopy.

Cells were permeabilized and nascent RNA was labeled with Br-UTP in synthesis buffer (50 mM Tris-HCl pH 7.4, 10 mM $MgCl_2$, 150 mM NaCl, 25 % glycerol, 0.5 mM PMSF, 25U/ml of RNasin, 1.8 mM ATP) supplemented with 0.5 mM CTP, GTP, and Br-UTP (Sigma) (15 min, room temperature). BrU-labeled RNA was detected using anti-BrdU antibody followed by Rhodamine Red™-X-conjugated goat anti-rabbit IgG and DAPI (4',6'-diamidino-2-phenylindole) staining. Nascent BrU-labeled RNA was observed by confocal microscope. For immunofluorescence confocal microscopy assays, cells were washed, fixed with 4% paraformaldehyde (15 min) and permeabilized with 0.5% Triton X-100 (15 min). They were incubated with the primary antibodies overnight at 4°C followed by incubating with the appropriate secondary antibody tagged with fluorescein isothiocyanate (FITC), Texas red, or Alexa 647 (Molecular Probes) (45 min, room temperature). Nuclei were stained with DAPI. Confocal fluorescence images were captured with an Olympus IX81 laser microscope. In all cases, optical sections were through the middle planes of the nuclei, as determined by nuclear counterstaining.

Immunoelectron Microscopy (Immuno-EM).

Cells were fixed with 2% paraformaldehyde containing 0.1% glutaraldehyde for 1 h, permeabilized with 0.5% Triton X-100 (15 min), and then incubated with 5% bovine serum albumin (15 min). Cells were incubated with the primary antibodies (overnight, 4°C) followed by incubating with gold particle-labeled secondary antibodies (Amersham Biosciences) (overnight, 4°C) for labeling. After post-fixation with 2% glutaraldehyde, cells were washed and stained with 1% Millipore-filtered uranyl acetate. The samples were dehydrated in increasing concentrations of ethanol, infiltrated, and embedded in Spurr's low viscosity medium. The samples were polymerized in a 70°C oven for 2 days.

The glass coverslips were removed by dipping in liquid nitrogen. Ultrathin sections were cut in a Leica Ultracut microtome (Leica, Deerfield, IL), stained with uranyl acetate and lead citrate in a Leica EM Stainer, and examined using a JEM 1010 transmission electron microscope (JEOL, USA, Inc., Peabody, MA) at an accelerating voltage of 80 kV. Digital images were obtained using an AMT Imaging System (Advanced Microscopy Techniques Corp, Danvers, MA).

Mass spectrometry.

Nuclear extracts of cells were immunoprecipitated with monoclonal anti-ErbB2 antibody as described above. The immunocomplexes were subjected to SDS-polyacrylamide gel electrophoresis and stained with Coomassie Blue. The protein bands on the PAGE were excised before in-gel digestion for Mass spectrometry analysis. Nanoscale capillary LC-MS/MS analysis was performed using an Ultimate capillary LC system (LC Packings, Amsterdam, The Netherlands) coupled to a QSTAR^{XL} quadrupole-time of flight (Q-TOF) mass spectrometer (Applied Biosystem/MDS Sciex, Foster City, CA). The nanoscale capillary LC separation was performed on a RP C18 column (15 cm, 75 μm i.d.). A nanoelectrospary interface was used for LC-MS/MS analysis. Ionization (2.0 kV ionization potential) was performed with a coated nanoLC tip. The nanoLC tip for on-line LC-MS used was a PicoTip (FS360-20-10-D-20; New Objective, Cambridge, MA). The optimum sprayer position was typically flush with or slightly inserted (about 1 mm) into the curtain chamber. The temperature of the heated laminar flow chamber was 100 ℃. The potential of the curtain plate was 250 V and the curtain gas was 1.3 L/min. Data acquisition was performed by automatic Information Dependent Acquisition (IDA; Applied Biosystem/MDS Sciex). The IDA automatically finds the most intense ions in a TOF MS spectrum, and then performs an optimized MS/MS analysis on the selected ions. The product ion spectra generated by nanoLC-MS/MS were searched against NCBI databases for exact matches using the ProID (Applied Biosystem/MDS Sciex) and the MASCOT search programs. A Homo sapiens

taxonomy restriction was used, and the mass tolerance of both precursor ion and fragment ions was 0.3 Da. Carbamidomethyl cysteine was a fixed modification, while oxidized methionine, histidine and tryptophan were variable modifications.

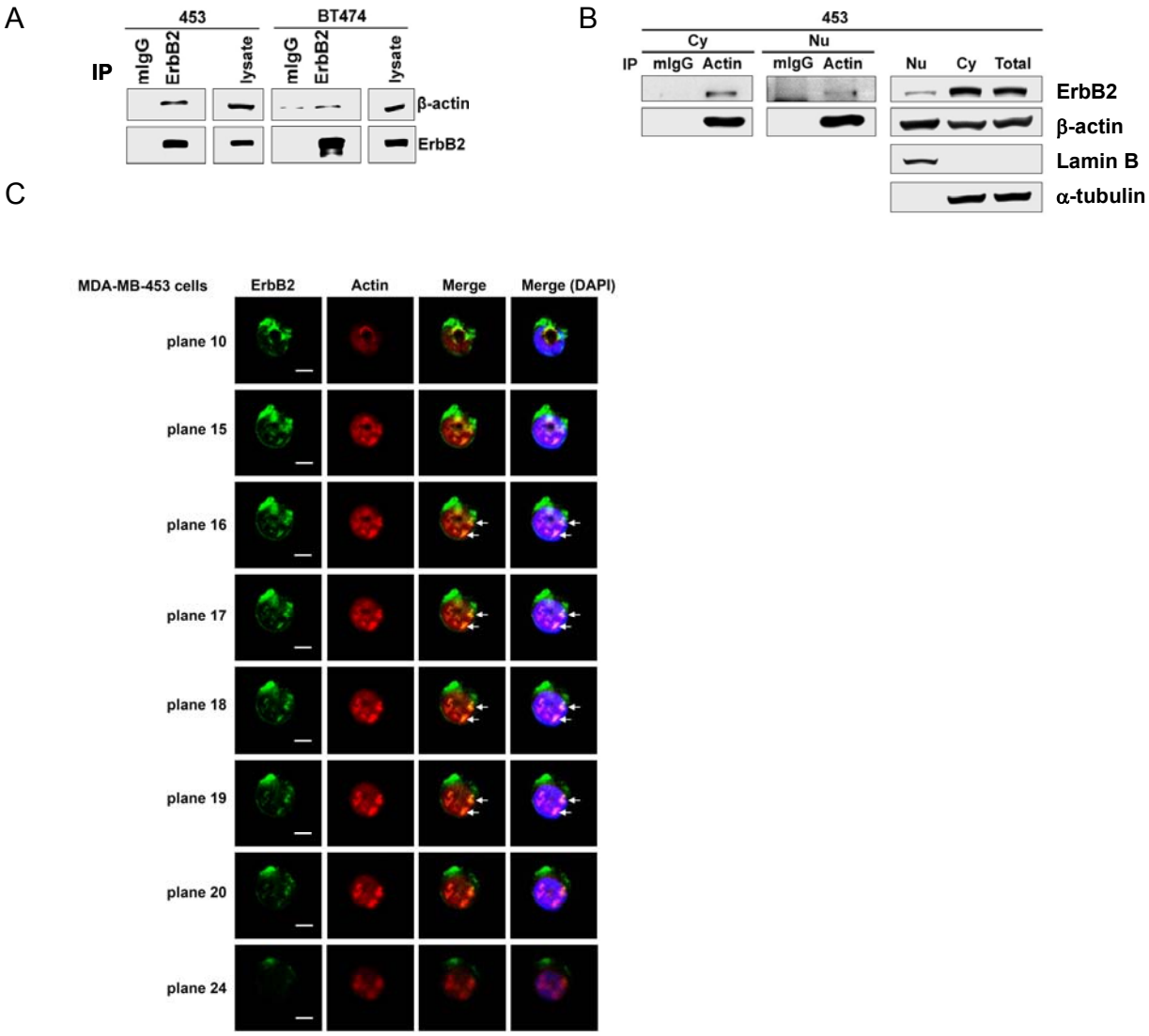

Figure. S1. ErbB2 associates and colocalizes with β-actin in multiple cells. (A-B) ErbB2 associates with β-actin both in the cytoplasm and the nucleus. Total cell lysates (A) and cytoplasmic (Cy) and nuclear (Nu) lysates (B) from MDA-MB-453 and BT474 cells were immunoprecipitated (IP) using antibodies against ErbB2, β-actin, or mouse IgG (mIgG); and then immunoblotted with antibodies as indicated. The cellular fractionation efficiency was also examined by antibodies against α-tubulin and lamin B. (C) Sub-nuclear localization of the ErbB-2 and β-actin in MDA-MB-453 cells using confocal analyses of ErbB2 (green), β-actin (red) and nuclei (DAPI staining, blue). For confocal microscopy, the cell was dissected into 33 focal planes with a thickness of 0.5 μm each. The nucleus spanned across focal plane 7 to plane 25. The middle plans (planes 15-20) within the nucleus are presented displaying from the top (plane 10) to the bottom (plane 24) of a particular group of ErbB-2 (green)-β-actin (red) complexes whose colocalization was indicated by white arrows in the merged images. Scale bar, 5 μm.

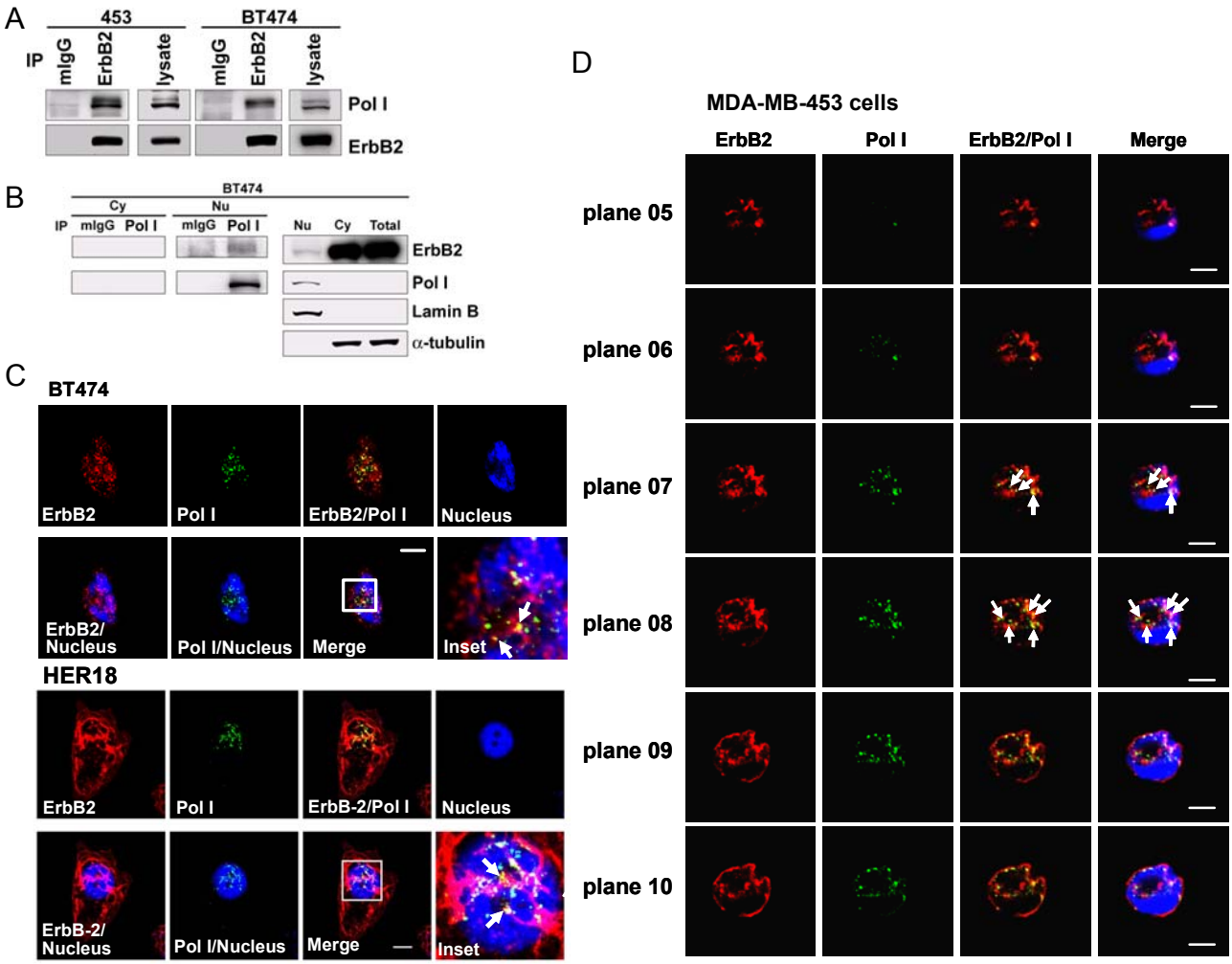

Figure. S2. ErbB2 associates and colocalizes with RNA Pol I in multiple cells. (A-B) ErbB2 associates with RNA Pol I. Total cell lysates (A) and cytoplasmic (Cy) and nuclear lysates (Nu) (B) from MDA-MB-453 and BT474 cells were immunoprecipitated (IP) with anti-ErbB2, anti-RNA Pol I, or mIgG antibodies, and analyzed by western blotting using antibodies as indicated. The cellular fractionation efficiency was also examined by antibodies against α-tubulin and lamin B. (C) ErbB2 (red) and RNA Pol I (green) colocalize in the nucleus (blue) of BT474 cells and the MCF-7 stable cell line expressing wild-type ErbB2 (HER18) using confocal microscopy as in Supplemental Figure 1C. The insets are shown in enlarged image. Scale bar, 10 μm. Arrows in the insets indicate nuclear colocalization. (D) Sub-nuclear localization of the ErbB-2 and RNA Pol I in MDA-MB-453 cells using confocal analyses of ErbB2 (red), RNA Pol I (green) and nuclei (DAPI staining, blue). For confocal microscopy, the cell was dissected into 25 focal planes with a thickness of 0.5 μm each. The nucleus spanned across focal plane 3 to plane 19. The middle plans (planes 5-10) within the nucleus are presented displaying from the top (plane 5) to the bottom (plane 10) of a particular group of ErbB-2 (red)-RNA Pol I (red) complexes whose colocalization was indicated by white arrows in the merged images. Scale bar, 5 μm.

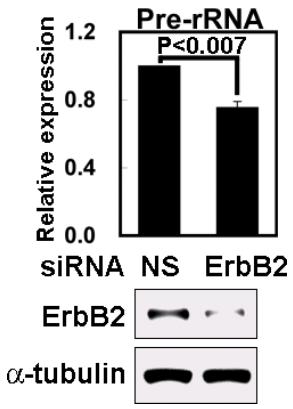

Figure. S3. Knockdown of ErbB2 using siRNA inhibits pre-rRNA synthesis in MDA-MB-453 cells
Cells transfected with ErbB2 or non-specific (NS) siRNAs were assessed for 45S pre-rRNA synthesis by RT-qPCR (top) and ErbB2 protein expression by western blotting using α-tubulin as control (bottom). The bars are presented as mean with SD (n=3). *p* value was analysed by Student's t test.

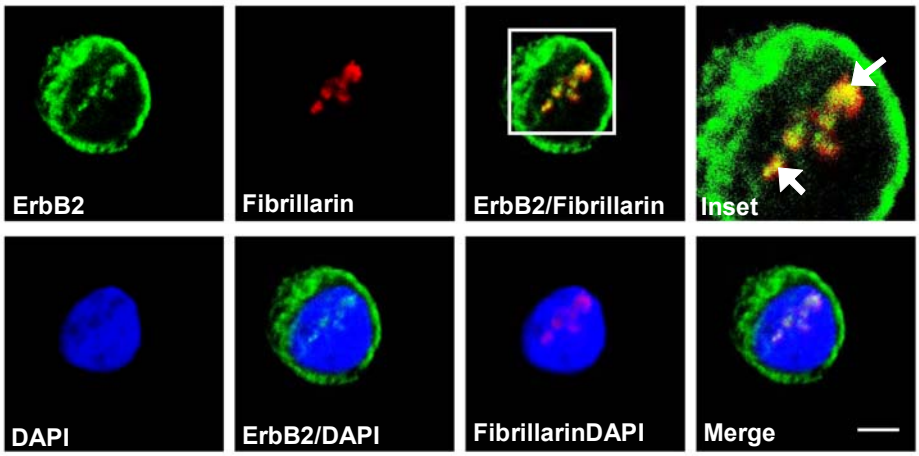

Figure. S4. ErbB2 colocalizes with nucleolar marker fibrillarin in the nucleolus of MDA-MB-453 cells using confocal analyses of ErbB2 (green), fibrillarin (red) and nuclei (DAPI staining, blue)
The inset is shown in enlarged image. Scale bar, 5 μm. Arrows in the insets indicate nucleolar colocalization.

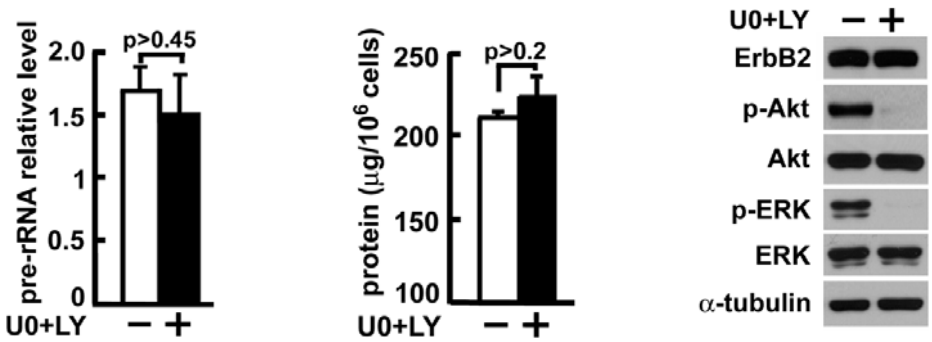

Figure. S5. ErbB-2-potentiated RNA Pol I transcription is independent of PI3-K and ERK activities. MCF-7 stable cell line expressing wild-type ErbB2 (HER18 cells) were treated with (+) or without (-) PI3-K inhibitor LY294002 and MEK inhibitor U0126 (U0+LY) for 4 hours and analyzed for 45S pre-rRNA synthesis (left) and total protein synthesis (middle) as in Figure 6B. Expression of ErbB-2, total Akt, phosphorylated Akt (p-Akt), total ERK, phosphorylated ERK (p-ERK), and α-tubulin proteins was analyzed by Western blotting as indicated (right).